Available online at www.sciencedirect.com
ScienceDirect
C. R. Mecanique 337 (2009) 15–23
COMPTES RENDUS MECANIQUE

Computation of a three-dimensional turbulent flow in a square duct using a cubic eddy-viscosity model

Honoré Gnanga, Hassan Naji, Gilmar Mompean *

Université Lille 1 – sciences et technologies, Polytech'Lille, LML – UMR CNRS 8107, boulevard Paul-Langevin, 59655 Villeneuve d'Ascq, France

Received 19 December 2008; accepted 5 January 2009

Presented by Olivier Pironneau

Abstract

The aim of this note is an evaluation of a cubic eddy-viscosity turbulent model. The study is carried out in square duct. This configuration presents a secondary flow and a significant anisotropy between the Reynolds stress components. In order to handle wall-proximity effects in the near-wall region, damping functions are introduced. The comparison of the modified model results with DNS and LES simulations shows good agreements. In particular, the mean secondary velocity and the mean streamwise vorticity are well predicted. ***To cite this article: H. Gnanga et al., C. R. Mecanique 337 (2009).***

Résumé

Prédiction d'un écoulement turbulent tridimensionnel dans une conduite à section carrée à l'aide d'un modèle cubique à viscosité turbulente. L'objectif de ce travail est l'évaluation d'un modèle non-linéaire cubique de turbulence. L'étude menée concerne l'écoulement turbulent dans une conduite à section carrée, configuration qui présente d'une part, une anisotropie importante entre les composantes du tenseur de Reynolds et d'autre part, un écoulement secondaire. Les effets de paroi sont pris en compte via des fonctions d'amortissement. La comparaison des résultats obtenus montre un bon accord avec ceux des simulations directes et des grandes échelles de la littérature. En particulier, l'écoulement secondaire et la vorticité longitudinale sont bien prédits. ***Pour citer cet article : H. Gnanga et al., C. R. Mecanique 337 (2009).***

Keywords: Turbulence; Non-linear models; Anisotropy; Computational fluid mechanics; Square duct flow

Mots-clés : Turbulence ; Modèle non linéaires ; Anisotropie ; Mécanique des fluides numérique ; Écoulement en conduite carrée

Version française abrégée

La prédiction numérique des écoulements turbulents est devenue un outil précieux qui permet d'obtenir une description détaillée de ces écoulements. Les tentatives pour prédire les caractéristiques turbulentes ont abouti à plusieurs

* Corresponding author.
E-mail address: gilmar.mompean@polytech-lille.fr (G. Mompean).

1631-0721/$ – see front matter
doi:10.1016/j.crme.2009.02.001

méthodes de prédétermination par voies numérique. Parmi celles-ci, on peut citer les méthodes de simulation directe (DNS), des grandes échelles (LES) et de fermetures des équations de Reynolds moyennées. (RANS). Le principe de cette dernière démarche est basé sur un traitement statistique des équations de Navier–Stokes avant toute résolution numérique. Toutefois, lors de l'utilisation de cette approche, son succès est fortement lié à la modélisation du tenseur de Reynolds. Il est maintenant admis que, sans modification, les modèles conventionnels à viscosité turbulente sont incapables de reproduire fidèlement le comportement des écoulements secondaires. Les modèles au second ordre (RSM) apparaissent ainsi comme le niveau d'approximation le plus naturel dans le contexte d'un traitement statistique des équations de Navier–Stokes en un point. Cependant, ces modèles sont très difficiles à résoudre, numériquement, pour des écoulements complexes tridimensionnels, car les termes modélisés requièrent une variété de fonctions de paroi et une estimation empirique des coefficients introduits dans ces modèles. Afin de combiner simplicité et efficacité, plusieurs modèles explicites à contraintes algébriques (EASM) ont été proposés. Ces modèles s'appuient sur une expression algébrique explicite du tenseur de Reynolds qui dépend des tenseurs taux de déformation et de rotation moyens et d'échelles scalaires caractéristiques de la turbulence. Ils peuvent prendre en compte l'anisotropie de la turbulence avec moins de temps de calculs et moins de place mémoire de stockage que les modèles RSM ou les approches DNS et LES et constituent ainsi une bonne alternative aux modèles RSM.

L'objectif de ce travail est la prédiction numérique d'écoulements turbulents tridimensionnels de fluide newtonien et incompressible à l'aide d'un modèle non-linéaire de turbulence proposé par Craft et al. [5]. Ce modèle prend en compte les effets de courbures des lignes de courant et est applicable dans la sous-couche visqueuse adjacente à la paroi. Pour rendre compte des effets visqueux, certaines constantes empiriques sont considérées comme des fonctions du nombre de Reynolds turbulent.

L'étude est menée dans une conduite à section carrée, configuration qui présente d'une part, une anisotropie importante entre les composantes du tenseur de Reynolds et d'autre part, un écoulement secondaire qui prend naissance au sein de l'écoulement principal. Les effets visqueux importants dus à la présence des parois sont pris en compte via des fonctions d'amortissement. La méthode utilisée pour résoudre les équations de Reynolds moyennées est celle des volumes finis avec un maillage entrelacé où les termes d'advection sont évalués à l'aide du schéma du second ordre QUICK.

Les prédictions sont confrontées à la fois aux données des simulations numériques directes de Gavrilakis [1], de Huser et Biringen [2], aux simulations des grandes échelles de Madabhushi et Vanka [3] et Xu et Pollard [12] et aux expériences de Niederschulte [13] et de Gessner et Emery [14]. La comparaison des grandeurs moyennes et statistiques de l'écoulement prédites montre une bonne performance du modèle considéré dans cette étude. En particulier, l'écoulement secondaire et la vorticité longitudinale sont très bien prédits.

1. Introduction

Numerical predictions of turbulent flows have become a valuable tool to obtain a detailed description of the turbulent flows. Attempts to predict the turbulent characteristics have resulted in several computational approaches which can generally be classified as DNS (Direct Numerical Simulation), LES (Large Eddy Simulation) or RANS (Reynolds Averaged Navier–Stokes). The results from the DNS are very accurate and reveal valuable information on the turbulence structures [1,2]. Therefore, the DNS approach is limited to low Reynolds numbers. An alternative to the DNS approach is the technique of LES. The LES approach is a numerical technique used to solve the partial differential equations governing turbulent fluid flow [3,4]. Therefore, the LES approach requires less computational effort than DNS but more effort than those methods that solve the Reynolds-averaged Navier–Stokes equations (RANS). The RANS approach required for the derivation of the RANS equations from the instantaneous Navier–Stokes equations is the Reynolds decomposition. Reynolds decomposition refers to separation of the flow variable into the mean component and the fluctuating component. However, when using this approach, the success of computational results depends heavily on the choice of the Reynolds Stress Models. In this study, Explicit Algebraic Reynolds Stress Models (EARSM) are used. These EARSM models propose the relations between Reynolds stress tensor, mean rate of deformation and the vorticity tensors, and they are able to capture more characteristics of the turbulent flows (anisotropy, near-wall behaviour).

This work focuses on a numerical investigation of a low Reynolds number turbulent flow through a square duct with emphasis on an EARSM model. This EARSM model has been proposed by Craft et al. [5] to extend the applicability of many quadratic models. Note that this model is a cubic relation between the strain and vorticity tensor and the

stress tensor, and according these authors, it seems most appropriate to reflect the effects of curvature and swirling. Therefore, the present study aims at investigating the capability of this cubic viscosity turbulence model in the fully turbulence flow through a straight square duct. This square duct configuration has been frequently chosen by many authors [1–3] since it is a relatively simple geometry which provides a good case test to improve turbulence models. Note that, this flow is strongly anisotropic and involves a secondary flow in the cross-stream plane, which is absent in the case of a plane channel.

2. Governing equations

The mean turbulent flow of a viscous, incompressible, Newtonian fluid is considered. To deal with the turbulent flow, the Reynolds decomposition is used, where the instantaneous variables for the velocity and pressure field are decomposed into the addition of mean and fluctuating parts. The equations governing the mean velocity $\overline{U}_i$ and mean pressure $\overline{P}$ are obtained from the RANS equations:

$$\frac{\partial \overline{U}_i}{\partial x_i} = 0 \tag{1}$$

$$\frac{\partial \overline{U}_i}{\partial t} + \frac{\partial}{\partial x_j}\left(\overline{U}_i \overline{U}_j\right) = -\frac{1}{\rho}\frac{\partial \overline{P}}{\partial x_i} + \frac{\partial}{\partial x_j}\left(\nu \frac{\partial \overline{U}_i}{\partial x_j} - \overline{u_i' u_j'}\right) \tag{2}$$

where ρ is the fluid density, ν is the cinematic viscosity and the quantity $\overline{u_i' u_j'}$ is the Reynolds stress tensor.

To close the RANS equations (1) and (2), the cubic eddy-viscosity model of turbulence proposed in [5] is used. The most general expression retaining terms up to cubic level that satisfies the required symmetry and contraction properties, can be written as follows:

$$\begin{aligned}\overline{u_i' u_j'} = {} & \frac{2}{3}k\delta_{ij} - \nu_t S_{ij} \\ & + c_1 \frac{\nu_t k}{\tilde{\varepsilon}}\left(S_{ik}S_{jk} - \frac{1}{3}S_{kl}S_{kl}\delta_{ij}\right) + c_2 \frac{\nu_t k}{\tilde{\varepsilon}}(\Omega_{ik}S_{jk} + \Omega_{jk}S_{ik}) + c_3 \frac{\nu_t k}{\tilde{\varepsilon}}\left(\Omega_{ik}\Omega_{jk} - \frac{1}{3}\Omega_{kl}\Omega_{kl}\delta_{ij}\right) \\ & + c_4 \frac{\nu_t k^2}{\tilde{\varepsilon}^2}(S_{ki}\Omega_{lj} + S_{kj}\Omega_{li})S_{kj} + c_5 \frac{\nu_t k^2}{\tilde{\varepsilon}^2}\left(\Omega_{il}\Omega_{lm}S_{mj} + S_{il}\Omega_{lm}\Omega_{mj} - \frac{2}{3}S_{lm}\Omega_{mn}\Omega_{nl}\delta_{ij}\right) \\ & + c_6 \frac{\nu_t k^2}{\tilde{\varepsilon}^2}S_{ij}S_{kl}S_{kl} + c_7 \frac{\nu_t k^2}{\tilde{\varepsilon}^2}S_{ij}\Omega_{kl}\Omega_{kl}\end{aligned} \tag{3}$$

where k $(= \overline{u_i' u_j'}/2)$ is the turbulent kinetic energy, ν_t $(= C_\mu k^2/\tilde{\varepsilon})$ is the turbulent viscosity, $\tilde{\varepsilon}$ $(= \varepsilon - 2\nu(\partial k^{1/2}/\partial x_j)^2)$ is the "isotropic" dissipation rate, δ_{ij} is the Kronecker tensor, and S_{ij} and Ω_{ij} are the mean rate of deformation and vorticity tensors.

The model coefficients $C_1, C_2, C_3, C_4, C_5, C_6, C_7$ of Eq. (3) are given in Table 1, where the coefficient C_μ is a function of the strain and vorticity invariants $\widetilde{S}$ and $\widetilde{\Omega}$:

$$C_\mu = 0.3/\left(1 + 0.35\left(\max\left(\widetilde{S}, \widetilde{\Omega}\right)\right)\right)^{3/2} \times \left(1 - \exp\left(-0.36\exp\left(0.75\left(\max\left(\widetilde{S}, \widetilde{\Omega}\right)\right)\right)\right)\right) \tag{4}$$

The dimensionless strain rate $\widetilde{S}$ and vorticity $\widetilde{\Omega}$ are denoted by:

$$\widetilde{S} = k/\tilde{\varepsilon}\sqrt{S_{ij}S_{ij}/2}, \qquad \widetilde{\Omega} = k/\tilde{\varepsilon}\sqrt{\Omega_{ij}\Omega_{ij}/2} \tag{5}$$

The cubic stress–strain relation (3) adopted here presents some advantages. Indeed, the quadratic terms and strain/vorticity-dependent coefficients are responsible for the ability of non-linear models to capture anisotropy, and

Table 1
The proposed form for the coefficients of Eq. (3).

C_1	C_2	C_3	C_4	C_5	C_6	C_7
−0.1	0.1	0.26	$-10C_\mu^2$	0.	$-5C_\mu^2$	$5C_\mu^2$

Table 2
Coefficients in k and $\tilde{\varepsilon}$ equations.

$C_{\varepsilon 1}$	$C_{\varepsilon 2}$	σ_k	σ_ε
1.44	$1.92(1-0.3\exp(-Re_t^2))$	1.0	1.3

Table 3
Values of constants a and b used in the damping function f_μ.

	$\langle u^2\rangle$	$\langle v^2\rangle$	$\langle w^2\rangle$	$-\langle uv\rangle$	$-\langle uw\rangle$	$-\langle vw\rangle$
a	−4.5	0.34	0.34	1.01	1.01	0.68
b	0.038	0.05	0.05	0.04	0.04	0.043

the cubic terms can reflect the effect of curvature. Also, theses cubic terms can capture the swirling effect. It is interesting to note that this model is not objective, as it uses the vorticity tensor Ω. We have used this model in a square duct without rotation, and the influence of the rotation given by the secondary flow is very weak as tested in previous work [6].

The turbulent energy k and the "isotropic" dissipation rate $\tilde{\varepsilon}$ are obtained from the following transport equations:

$$\frac{Dk}{Dt} = P_k - \varepsilon + \frac{\partial}{\partial x_j}\left[\left(\nu + \frac{\nu_t}{\sigma_k}\right)\frac{\partial k}{\partial x_j}\right] \tag{6}$$

$$\frac{D\tilde{\varepsilon}}{Dt} = c_{\varepsilon 1}\frac{\tilde{\varepsilon}}{k}P_k - c_{\varepsilon 2}\frac{\tilde{\varepsilon}^2}{k} + E + Y_{ap} + \frac{\partial}{\partial x_j}\left[\left(\nu + \frac{\nu_t}{\sigma_\varepsilon}\right)\frac{\partial \tilde{\varepsilon}}{\partial x_j}\right] \tag{7}$$

where $D(\cdot)/Dt = \partial(\cdot)/\partial t + \overline{U}_j\partial(\cdot)/\partial x_j$ is the material derivative, $P_k = \overline{u_i u}_j\partial\overline{U}_i/\partial x_j$ is the turbulent production. The near-wall source term E, takes the form $2\nu\nu_t(\partial^2\overline{U}_i/\partial x_j\partial x_k)^2$, is here modified to reduce its dependence on Reynolds number. Consequently, it is modelled as follows:

$$\begin{cases} E = 0.0022\dfrac{\widetilde{S}\nu_t k^2}{\tilde{\varepsilon}}\left(\dfrac{\partial^2\overline{U_i}}{\partial x_j\partial x_k}\right)^2 & \text{if } Re_t \leqslant 250 \\ E = 0 & \text{if } Re_t > 250 \end{cases} \tag{8}$$

The length-scale correction Y_{ap} can be expressed as follows:

$$Y_{ap} = 0.83\frac{\tilde{\varepsilon}^2}{k}\max\left(\left[\frac{k^{1.5}}{2.5\tilde{\varepsilon}y} - 1\right]\left[\frac{k^{1.5}}{2.5\tilde{\varepsilon}y}\right]^2, 0\right) \tag{9}$$

The various coefficients are given in Table 2.

To enable a correct behaviour in the regions close to the walls, damping functions of Van Driest types [7] have been used. These functions are:

$$f = \left(1 - a\exp(-bz^+)\right)\left(1 - a\exp(-by^+)\right) \tag{10}$$

where z^+ $(= zu_\tau/\nu)$ and y^+ $(= yu_\tau/\nu)$ are the non-dimensional coordinates scaled by the kinematic viscosity ν and the mean frictional velocity $u_\tau = (\tau_w/\rho)^{1/2}$, τ_w being the mean wall shear stress. The constants a and b suggested here (see Table 3) are those that best describes the pattern of the flow near the corner. These constants have been calibrated using the a priori technique, with the mean field turbulent coming from DNS data [1]. Information about this calibration can be found in [8]. These damping functions type were previously used by [6,9] and [10]. From Table 3, one can note that all the normalised Reynolds stresses $\langle u_i u_j\rangle$ $(= \overline{u_i' u_j'}/u_\tau^2)$ have different damping functions.

3. Numerical method

The governing equations are spatially discretized using a second-order finite volume method on a staggered grid. The conservation equations are integrated over a control volume, and the Gauss theorem is used to transform the volume integrals into surface integrals. The pressure, the turbulent kinetic energy, the "isotropic" dissipation rate and the normal Reynolds stress components are treated in the centre of the control volumes; the velocities are computed

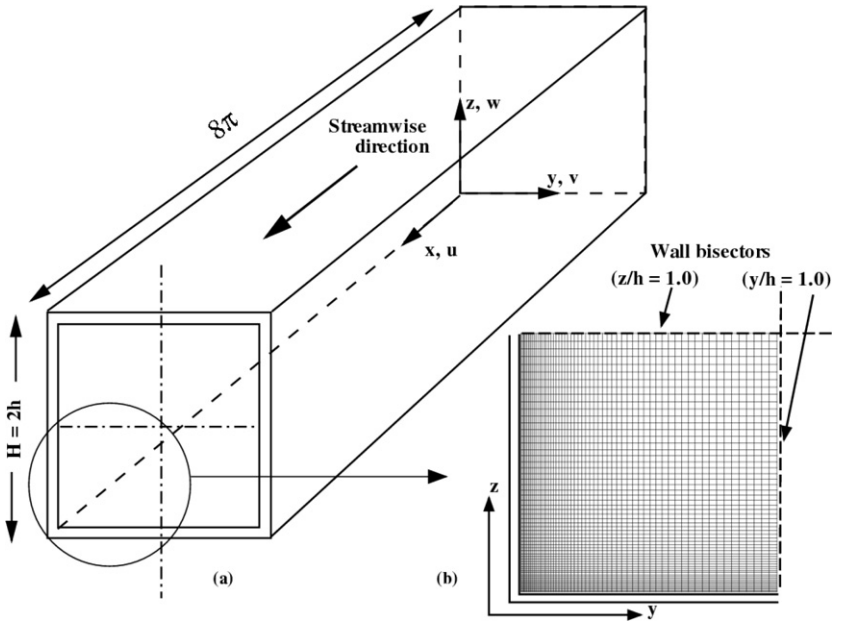

Fig. 1. (a) Flow geometry and axes system; (b) Quadrant of the square.

in the centre of the faces and the cross components of the Reynolds tensor are attached to nodes located at the mid-edges. The convective terms are approximated by the quadratic upstream interpolation scheme (QUICK). Also, the mass conservation equation is evaluated at the time $n+1$, whereas the advection and diffusion terms in the moment equation are evaluated at the time n. Owing to the explicit treatment of the advection terms, the time step Δt was restricted to the CFL condition.

The decoupling procedure for the pressure is derived from the Mark and Cell (MAC) algorithm.

The geometrical configuration of the square duct with the reference axes is shown in Fig. 1. The cross-section is divided into four quadrants. Because of symmetry, only quadrant of the square need to be calculated with symmetry conditions at the wall bisectors.

For the first time-step, at the inlet of the duct, a constant profile was given to $\overline{U}$, k and ε. The secondary velocities were initialised as nil (and) all over the domain. The k and ε inlet values were obtained from the DNS data using the rsm (root mean square) velocities and the eddy viscosity, that was about four times the molecular viscosity. At the outlet, a homogeneous Neumann boundary condition was used for the inlet condition. The same procedure is used for the following time-steps up to convergence.

The Reynolds number of 4600 is based on the bulk velocity and the hydraulic diameter of the duct. The calculations were carried out using 63×63 grid points, regularly spaced in the cross-section and 120 grid points in the streamwise direction. The outcome with this grid points was found to be satisfactory.

The grid convergence was checked using 61×61 grid points in the cross-section, the maximum difference observed between the two calculations were less than 1% in the streamwise velocity near the corner. Mesh independence for the results has been verified with different meshes.

The boundary condition values for k and ε, at the first grid point near the wall, was calculated taking into account the fact that this point was in the viscous sub-layer. Also, due to the use of a staggered grid, the value of k and ε are not defined at the wall. In this paper, we consider the following boundary conditions for the equation of k and ε, which have been used by [11].

A condition for symmetry, homogeneous Neumann, was used for all the variables along the wall bisectors of the square duct.

4. Results

The contours of mean streamwise velocity and secondary flow vectors in a quadrant of a cross-section are shown in Figs. 2 and 3, respectively.

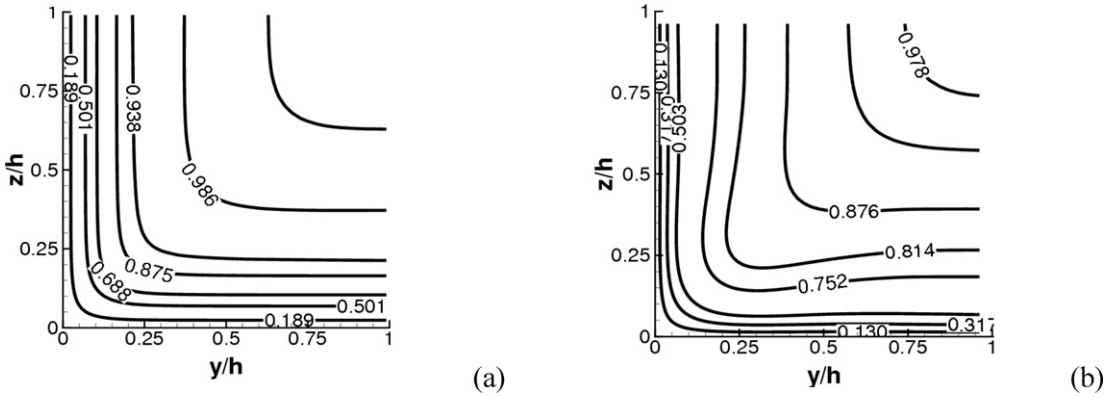

Fig. 2. Contours of the normalised mean streamwise velocity $\overline{U}/\overline{U}_0$ in a quadrant. (a) Present study; (b) DNS data [1].

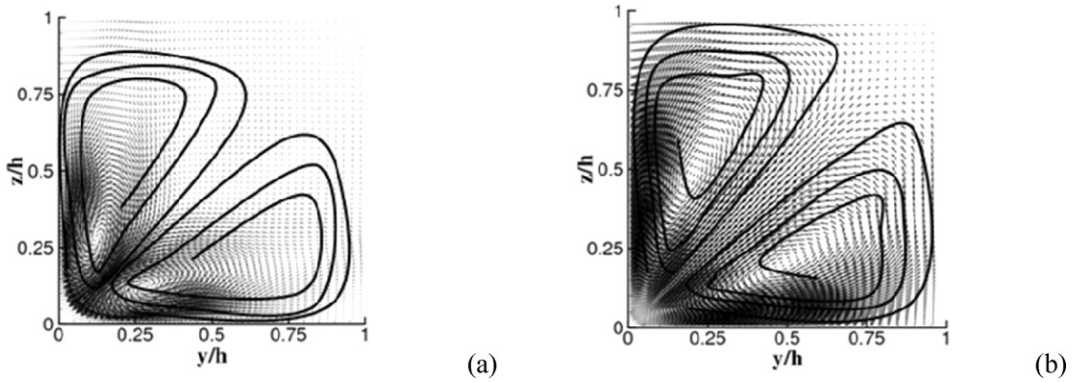

Fig. 3. Mean secondary velocity vectors. (a) Present study; (b) DNS data [1].

The mean streamwise velocity and secondary flow vectors from DNS data by [1] are also given for comparison. By the examination of Fig. 2, as expected the flow is symmetric according to the corner bisector, and the prediction is in good agreement with DNS data. The secondary velocities convect mean-flow momentum from the central region to the corner region along the corner bisectors. They also transport the low-momentum fluid to the center along the wall bisector. This results in the bulging of the streamwise-velocity contours towards the corner which can be seen in Fig. 2. It should be noted that the mean secondary velocity from the present RANS is weaker than those from DNS data by [1].

The mean streamwise and normal velocities along the z direction at different sections, namely, at $y/h = 0.3$, $y/h = 0.7$ and $y/h = 1.0$ are presented in Fig. 4. It can be seen in these figures that the mean velocities from the present study agree well with DNS data by [1,2] and LES data by [12]. However, experimental data by [13] and by [14] causes a noticeable discrepancy in the region away from the wall (at section $y/h = 1.0$). Also at section $y/h = 0.3$, the DNS data show a strong distortion on the mean streamwise velocity induced by the secondary flow.

Contours of mean streamwise vorticity are shown in Fig. 5. This quantity is a direct manifestation of the secondary flow. Again, there is very good qualitative agreement between the present RANS results and the DNS data by [1].

Fig. 6 shows three components of turbulence intensity normalised by the local friction velocity along the wall bisector. In this figure, DNS data by [1,2], LES data by [3,12], and experimental data by [13], are provided for comparison with the present RANS data. It can be seen in this figure that the turbulence intensities u_{rms} and v_{rms} from the present RANS data agree well with DNS data by Gavrilakis [1], Huser and Biringen [2] and with measured data by Niederschulte [13]. Also, it is observed that the profiles of turbulence intensity w_{rms} well predict the DNS results. The profile of this turbulence intensity from the present RANS appears to be slightly larger than the profile from LES data by [12], and experimental data by [13].

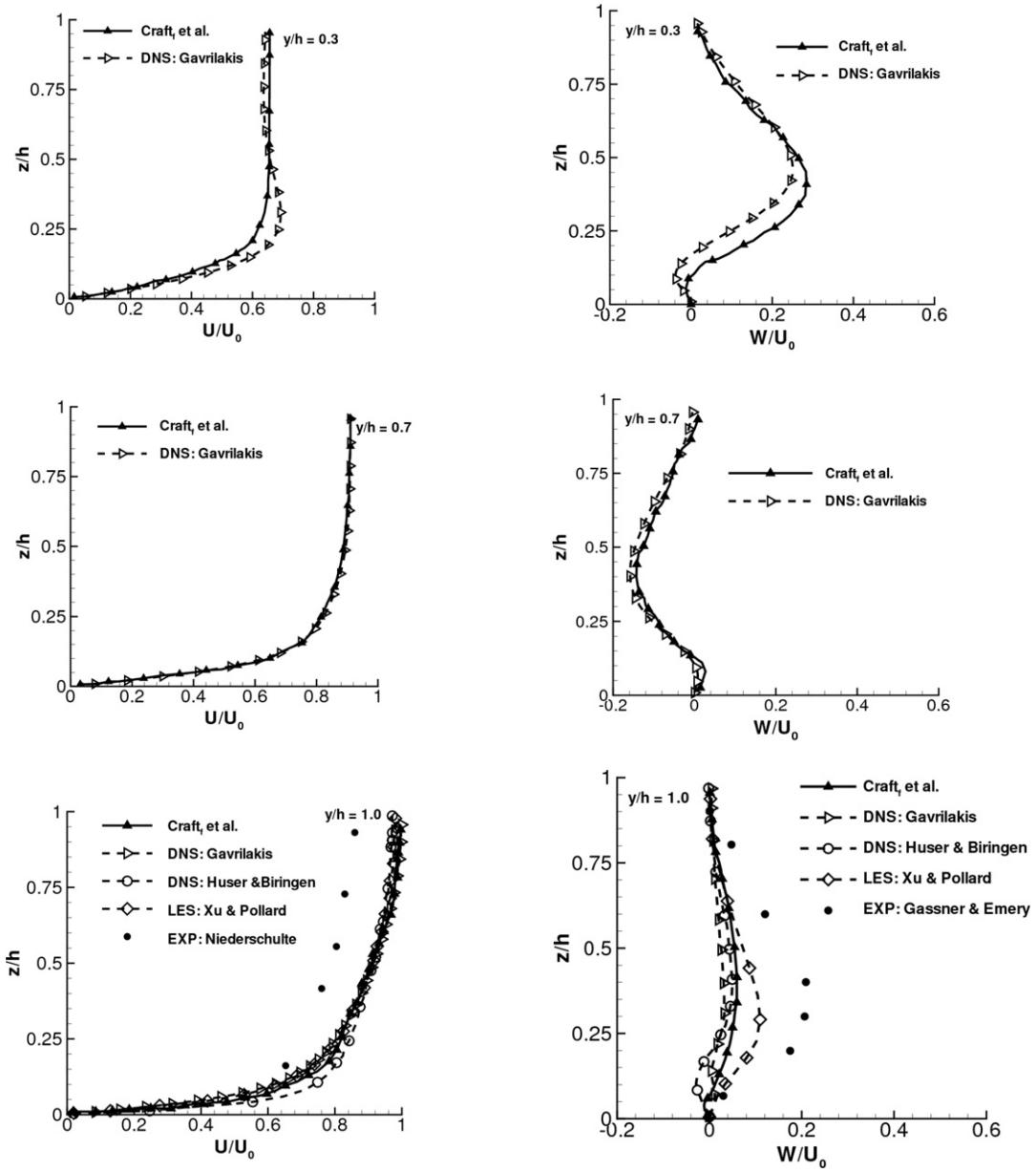

Fig. 4. The normalised mean velocity at different sections $y/h = 0.3$, 0.7 and 1.0. Streamwise velocity $\overline{U}/\overline{U}_0$ (left); Normal velocity $\overline{W}/\overline{U}_0$ (right).

5. Conclusion

A numerical simulation of the turbulent flow through a square duct was performed using the non-linear model proposed by Craft et al. [5]. To predict the significant viscous effects due to the presence of the wall and corner, damping functions are implemented. The simulations results were compared with DNS data by [1,2], LES data by [3,12], and with measured data by [13,14]. The present RANS turns out to be able to correctly reproduce both the mean flow properties and turbulence statistics. Indeed, the profiles and maps of the mean velocity and turbulence statistics are in good agreement with the DNS, LES and experimental data in particular when one approaches the centre of the duct. Also, our RANS simulations, which are performed at a significantly reduced computational cost compared with DNS and LES, well reproduce the intensity of the secondary flow and the mean streamwise vorticity.

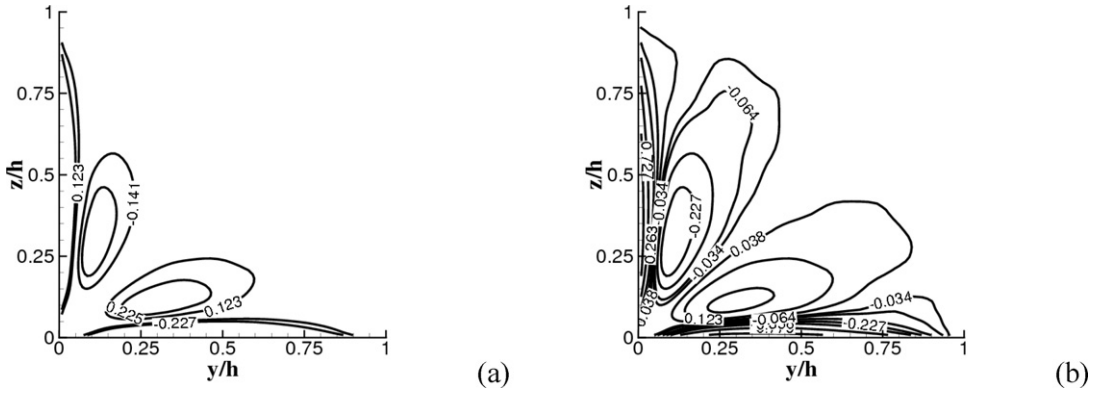

Fig. 5. Distribution of the mean streamwise vorticity. (a) Present study; (b) DNS data [1].

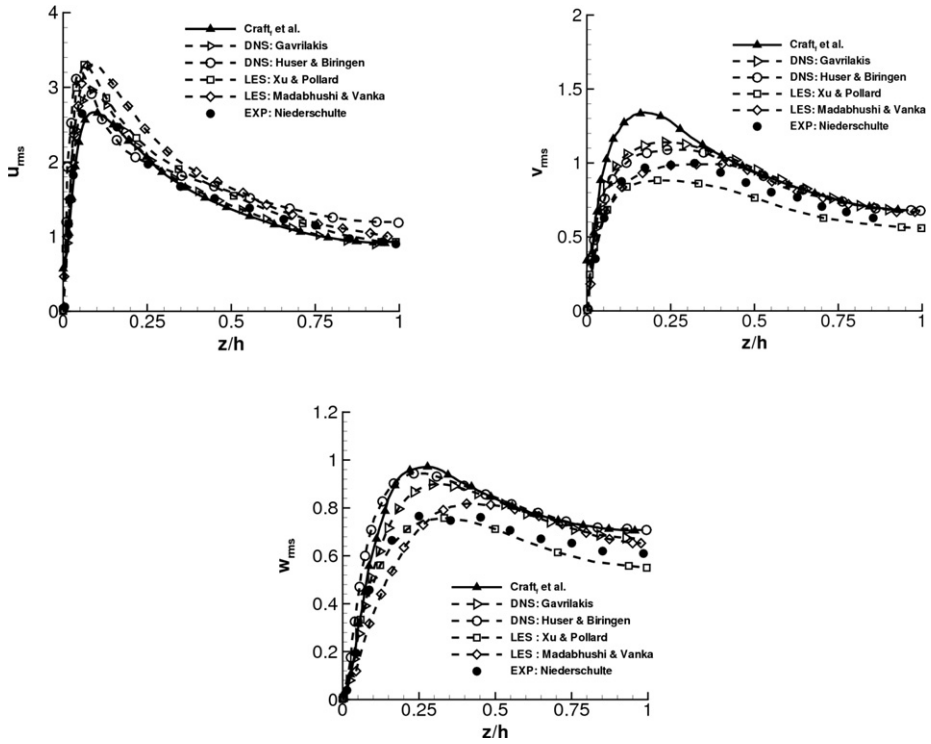

Fig. 6. Turbulence intensities at the wall bisector ($y/h = 1.0$).

References

[1] S. Gavrilakis, Numerical simulation of low-Reynolds-number turbulent flow through a straight square duct, J. Fluid Mech. 224 (1992) 101–129.

[2] A. Huser, S. Biringen, Direct numerical simulation for turbulent flow in a square duct, J. Fluid Mech. 257 (1993) 65–95.

[3] R.K. Madabhushi, S.P. Vanka, Large-eddy simulation of turbulence-driven secondary flow in a square duct, Phys. Fluids A 3 (11) (1991) 2734–2745.

[4] M.S. Vasquez, O. Métais, Large eddy simulation of the turbulent flow though a heath square duct, J. Fluid Mech. 453 (2002) 201–238.

[5] T.J. Craft, B.E. Launder, K. Suga, Development and application of the cubic eddy-viscosity model of turbulence, Int. J. Heat Fluid Flow 17 (1996) 108–115.

[6] H. Naji, G. Mompean, O. El Yahyaoui, Evaluation of explicit algebraic stress models using direct numerical simulations, J. Turbulence 5 (2004) 38–63.

[7] E.R. Van Driest, On turbulent flow near a wall, J. Aeronaut. Sci. 23 (1956) 1007–1011.

[8] H. Gnanga, Analyse numérique d'écoulements turbulents anisotropes à l'aide de modèles non-linéaires de turbulence, Ph.D. thesis, Université des Sciences et Technologies de Lille, France, 2008.
[9] G. Mompean, Numerical simulation of a turbulent flow near a right-angled corner using the Speziale non-linear model with RNG k–ε equations, Computers and Fluids 7 (1997) 847–852.
[10] S. Nasizima, A numerical study of turbulent square-duct flow using an anisotropic k–ε model, Theoret. Comput. Fluid Dynam. 2 (1990) 61–72.
[11] C.V. Patel, W. Rodi, G. Scheuerer, Turbulence models for near-wall and low Reynolds number flows: a review, AIAA J. 23 (1984) 1308–1319.
[12] H. Xu, A. Pollard, Large eddy simulation of turbulence flow in square annular duct, Phys. Fluids 13 (2001) 3321–3337.
[13] M.A. Niederschulte, Turbulent flow through a rectangular channel, Ph.D. thesis, Univ. of Illinois at Urbana-Champaign, III, 1989.
[14] F.B. Gessner, A.F. Emery, The numerical prediction of developing flow in rectangular ducts, ASME Trans. J. Fluids Eng. 103 (1981) 445–455.